

Branching fraction measurements of $\psi(2S)$ decay to baryon-antibaryon final states

T. K. Pedlar,¹ D. Cronin-Hennessy,² K. Y. Gao,² D. T. Gong,² J. Hietala,² Y. Kubota,² T. Klein,² B. W. Lang,² S. Z. Li,² R. Poling,² A. W. Scott,² A. Smith,² S. Dobbs,³ Z. Metreveli,³ K. K. Seth,³ A. Tomaradze,³ P. Zweber,³ J. Ernst,⁴ A. H. Mahmood,⁴ H. Severini,⁵ D. M. Asner,⁶ S. A. Dytman,⁶ W. Love,⁶ S. Mehrabyan,⁶ J. A. Mueller,⁶ V. Savinov,⁶ Z. Li,⁷ A. Lopez,⁷ H. Mendez,⁷ J. Ramirez,⁷ G. S. Huang,⁸ D. H. Miller,⁸ V. Pavlunin,⁸ B. Sanghi,⁸ I. P. J. Shipsey,⁸ G. S. Adams,⁹ M. Cravey,⁹ J. P. Cummings,⁹ I. Danko,⁹ J. Napolitano,⁹ Q. He,¹⁰ H. Muramatsu,¹⁰ C. S. Park,¹⁰ W. Park,¹⁰ E. H. Thorndike,¹⁰ T. E. Coan,¹¹ Y. S. Gao,¹¹ F. Liu,¹¹ M. Artuso,¹² C. Boulahouache,¹² S. Blusk,¹² J. Butt,¹² O. Dorjkhaidav,¹² J. Li,¹² N. Menaa,¹² R. Mountain,¹² R. Nandakumar,¹² K. Randrianarivony,¹² R. Redjimi,¹² R. Sia,¹² T. Skwarnicki,¹² S. Stone,¹² J. C. Wang,¹² K. Zhang,¹² S. E. Csorna,¹³ G. Bonvicini,¹⁴ D. Cinabro,¹⁴ M. Dubrovin,¹⁴ R. A. Briere,¹⁵ G. P. Chen,¹⁵ J. Chen,¹⁵ T. Ferguson,¹⁵ G. Tatishvili,¹⁵ H. Vogel,¹⁵ M. E. Watkins,¹⁵ J. L. Rosner,¹⁶ N. E. Adam,¹⁷ J. P. Alexander,¹⁷ K. Berkelman,¹⁷ D. G. Cassel,¹⁷ V. Crede,¹⁷ J. E. Duboscq,¹⁷ K. M. Ecklund,¹⁷ R. Ehrlich,¹⁷ L. Fields,¹⁷ L. Gibbons,¹⁷ B. Gittelman,¹⁷ R. Gray,¹⁷ S. W. Gray,¹⁷ D. L. Hartill,¹⁷ B. K. Heltsley,¹⁷ D. Hertz,¹⁷ C. D. Jones,¹⁷ J. Kandaswamy,¹⁷ D. L. Kreinick,¹⁷ V. E. Kuznetsov,¹⁷ H. Mahlke-Krüger,¹⁷ T. O. Meyer,¹⁷ P. U. E. Onyisi,¹⁷ J. R. Patterson,¹⁷ D. Peterson,¹⁷ E. A. Phillips,¹⁷ J. Pivarski,¹⁷ D. Riley,¹⁷ A. Ryd,¹⁷ A. J. Sadoff,¹⁷ H. Schvarthoff,¹⁷ X. Shi,¹⁷ M. R. Shepherd,¹⁷ S. Stroiney,¹⁷ W. M. Sun,¹⁷ D. Urner,¹⁷ T. Wilksen,¹⁷ K. M. Weaver,¹⁷ M. Weinberger,¹⁷ S. B. Athar,¹⁸ P. Avery,¹⁸ L. Breva-Newell,¹⁸ R. Patel,¹⁸ V. Potlia,¹⁸ H. Stoeck,¹⁸ J. Yelton,¹⁸ P. Rubin,¹⁹ C. Cawfield,²⁰ B. I. Eisenstein,²⁰ G. D. Gollin,²⁰ I. Karliner,²⁰ D. Kim,²⁰ N. Lowrey,²⁰ P. Naik,²⁰ C. Sedlack,²⁰ M. Selen,²⁰ E. J. White,²⁰ J. Williams,²⁰ J. Wiss,²⁰ K. W. Edwards,²¹ and D. Besson²²

(CLEO Collaboration)

¹*Luther College, Decorah, Iowa 52101*

²*University of Minnesota, Minneapolis, Minnesota 55455*

³*Northwestern University, Evanston, Illinois 60208*

⁴*State University of New York at Albany, Albany, New York 12222*

⁵*University of Oklahoma, Norman, Oklahoma 73019*

⁶*University of Pittsburgh, Pittsburgh, Pennsylvania 15260*

⁷*University of Puerto Rico, Mayaguez, Puerto Rico 00681*

⁸*Purdue University, West Lafayette, Indiana 47907*

⁹*Rensselaer Polytechnic Institute, Troy, New York 12180*

¹⁰*University of Rochester, Rochester, New York 14627*

¹¹*Southern Methodist University, Dallas, Texas 75275*

¹²*Syracuse University, Syracuse, New York 13244*

¹³*Vanderbilt University, Nashville, Tennessee 37235*

¹⁴*Wayne State University, Detroit, Michigan 48202*

¹⁵*Carnegie Mellon University, Pittsburgh, Pennsylvania 15213*

¹⁶*Enrico Fermi Institute, University of Chicago, Chicago, Illinois 60637*

¹⁷*Cornell University, Ithaca, New York 14853*

¹⁸*University of Florida, Gainesville, Florida 32611*

¹⁹*George Mason University, Fairfax, Virginia 22030*

²⁰*University of Illinois, Urbana-Champaign, Illinois 61801*

²¹*Carleton University, Ottawa, Ontario, Canada K1S 5B6*

and the Institute of Particle Physics, Canada

²²*University of Kansas, Lawrence, Kansas 66045*

(Dated: December 2, 2024)

Abstract

Using 3.08 million $\psi(2S)$ decays observed in e^+e^- collisions by the CLEO detector, we present the results of a study of the $\psi(2S)$ decaying into baryon-antibaryon final states. We report the most precise measurements of the following eight modes: $p\bar{p}$, $\Lambda\bar{\Lambda}$, $\Xi^-\bar{\Xi}^-$, $\Xi^0\bar{\Xi}^0$ (first observation), $\Sigma^+\bar{\Sigma}^+$ (first observation), and $\Sigma^0\bar{\Sigma}^0$, and place upper limits for the modes, $\Xi^{*0}\bar{\Xi}^{*0}$ and $\Omega^-\bar{\Omega}^-$.

The study of $\psi(2S)$ production in e^+e^- and its subsequent decay into two hadrons provides a test of the predictive power of QCD [1], including information on gluon spin, quark distribution amplitudes in baryon-antibaryon pairs, and total hadron helicity conservation. The decays are predicted to proceed via the annihilation of the constituent $c\bar{c}$ into three gluons or a virtual photon. This model leads to the prediction that the ratio of the branching fraction into a specific final state to the branching fraction of the J/Ψ into that same state should be a constant value of approximately 13%, the corresponding ratio for the dilepton final state [2]. This rule, which was previously referred to as the “12% rule”, is roughly obeyed for several channels, but fails for others [3]. This Letter concentrates on the investigation of the two-body decays of the $\psi(2S)$ into a baryon-antibaryon pair. Previous measurements [4] of the $\psi(2S)$ decaying into these final states have very large statistical uncertainties. The CLEO [5] detector, with the advantage of good charged and neutral particle detection efficiencies, together with secondary and tertiary vertex reconstruction, gives us the opportunity to make the most precise measurements yet of these branching fractions.

The data used in this analysis were collected at the CESR e^+e^- storage ring, which has been reconfigured to run near $c\bar{c}$ threshold by inserting 6 wigglers [5]. Our analysis is based on 3.08×10^6 $\psi(2S)$ decays which corresponds to the total integrated luminosity of 5.63 pb^{-1} . Approximately half of the $\psi(2S)$ data (2.74 pb^{-1}) were taken with the CLEO III detector configuration [6] and the remainder (2.89 pb^{-1}) of the $\psi(2S)$ data, and all the continuum data (20.70 pb^{-1} , $\sqrt{s} = 3.67 \text{ GeV}$) were taken with the reconfigured CLEO-c detector [5]. We generated 10,000 Monte Carlo events using simulations of each of the two detector configurations for each of the eight decay modes, using a GEANT-based [7] detector modeling program. For all modes we generated Monte Carlo samples with a flat distribution in $\cos \theta$, where θ is the angle of the decay products in the center-of-mass system (in colliding beam experiments this angle is measured relative to the beam axis). For spin 1/2 baryons in the baryon octet, we then weighted the Monte Carlo samples with a $1 + \cos^2 \theta$ angular distribution, in agreement with the naive expectation. Possible deviations from these angular distributions will be one source of systematic uncertainty in our measurements.

We begin by reconstructing the hyperons in the following decay modes (branching fractions [4] are listed in parentheses): $\Lambda \rightarrow p\pi^-$ (63.9%), $\Sigma^+ \rightarrow p\pi^0$ (51.6%), $\Sigma^0 \rightarrow \Lambda\gamma$ (100.0%), $\Xi^- \rightarrow \Lambda\pi^-$ (99.9%), $\Xi^0 \rightarrow \Lambda\pi^0$ (99.5%), $\Xi^{*0} \rightarrow \Xi^-\pi^+$ (51.6%), and $\Omega^- \rightarrow \Lambda K^-$ (67.8%). To discriminate between protons, kaons, pions, and electrons, we combined specific ionization (dE/dx) measured in the drift chamber [6] and log-likelihoods obtained from the RICH sub-detector [6] to form a joint log-likelihood difference: $\mathcal{L}(p - \pi) = L_{RICH}(p) - L_{RICH}(\pi) + \sigma_{dE/dx}^2(p) - \sigma_{dE/dx}^2(\pi)$, where the more negative $\mathcal{L}(p - \pi)$, the higher the likelihood that the particle is a proton compared to a pion. Our requirement on these quantities varies in value from mode to mode depending upon background considerations. Further details of this procedure may be found elsewhere [8]. For protons in the $p\bar{p}$ and Σ^0 decay modes we require $\mathcal{L}(p - \pi) < -9$ and $\mathcal{L}(p - K) < -9$ (3 σ separation), and for those in the $p\bar{p}$ mode we require additional criteria $\mathcal{L}(p - e) < -9$ as, in this case alone, electrons are a potentially significant background. For protons that are the daughters of Λ decays we make the looser requirements of $\mathcal{L}(p - \pi) < 0$ and $\mathcal{L}(p - K) < 0$, which are both very efficient. Kaons from Ω^- decays are strongly identified with $\mathcal{L}(K - \pi) < -9$ and $\mathcal{L}(K - p) < -9$. Pions are only required to have energy loss measurements consistent with the pion identity. Photon candidates were identified in the CsI calorimeter.

The analysis procedure for reconstructing Λ and Ξ^- closely follows that presented ear-

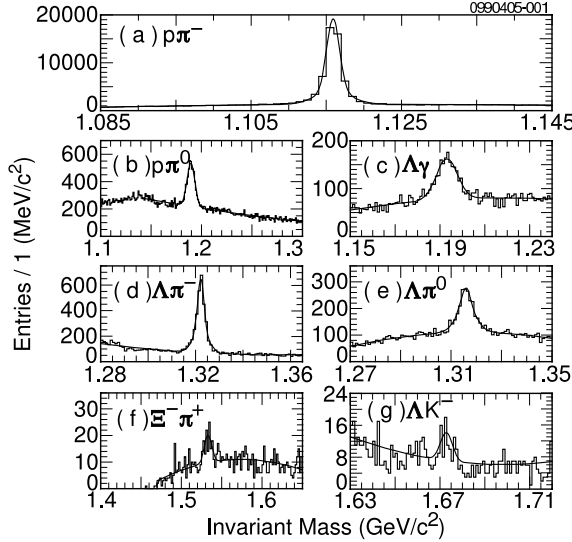


FIG. 1: Inclusive hyperon invariant mass distribution in $\psi(2S)$ data: (a) $\Lambda \rightarrow p\pi^-$, (b) $\Sigma^+ \rightarrow p\pi^0$, (c) $\Sigma^0 \rightarrow \gamma\Lambda$, (d) $\Xi^- \rightarrow \Lambda\pi^-$, (e) $\Xi^0 \rightarrow \Lambda\pi^0$, (f) $\Xi^{*0} \rightarrow \Xi^-\pi^+$, (g) $\Omega^- \rightarrow \Lambda K^-$.

lier [8]. The Ω^- reconstruction follows the steps of the Ξ^- reconstruction by replacing a pion by a kaon. Σ^0 hyperons are reconstructed by combining a Λ with a photon and requiring the photon energy in the crystal calorimeter to be in excess of 50 MeV, not matched to a charged track, and consistent in shape to that from a photon. Ξ^0 and Σ^+ hyperon reconstruction is complicated by the fact that there is no direction information from the CsI photon clusters for the π^0 reconstruction. A kinematic fit is made to the hypothesis that the parent hyperon started at the beamspot, and decayed after a positive pathlength to a decay vertex which is the origin of the $\pi^0 \rightarrow \gamma\gamma$ decay. A cut was placed on the χ^2 of the fit to this topology, which includes the fit to the π^0 mass from the newly found hyperon decay vertex. The Ξ^{*0} candidate is reconstructed by vertexing a positively charged pion candidate, consistent with coming from the beamspot, with the already found Ξ^- . All hyperon candidates were required to have vertices significantly separated from the beamspot, with the flight distance of the Λ measured from the parent (Ξ^0 , Ξ^- , or Ω^-) decay vertex, to be positive. In Figure 1 we show the inclusive hyperon yields in the $\psi(2S)$ data. We observed 48×10^3 Λ candidate events in the $\psi(2S)$ data as shown in Fig 1(a) with a fitted width (σ) found to be $1.53 \text{ MeV}/c^2$, consistent with Monte Carlo estimates. The fitted yields (widths) in Fig. 1(b) and (c) for Σ^+ and Σ^0 candidates are approximately 3×10^3 ($4.0 \text{ MeV}/c^2$) and 1×10^3 ($4.7 \text{ MeV}/c^2$), respectively. Invariant mass distributions for the Ξ^- and Ξ^0 are shown in Fig. 1(d) and (e), respectively. The fit yielded approximately 2.7×10^3 and 1.2×10^3 for the signal events and $2.4 \text{ MeV}/c^2$ and $3.6 \text{ MeV}/c^2$ for widths for the Ξ^- and Ξ^0 candidates, respectively. The fits in Fig. 1(f) and (g) yielded 115 ($4.69 \text{ MeV}/c^2$) and 47 ($2.69 \text{ MeV}/c^2$) events (width) for the Ξ^{*0} and Ω^- spin $3/2$ baryons. Hyperon candidates within 3σ of their nominal masses are considered for further analysis. We then combined the 4-momenta of these baryons with the corresponding 4-momenta of their charge conjugates and formed $\psi(2S)$ candidates.

We note that baryon-antibaryon pairs produced by $\psi(2S)$ decays have a back-to-back topology, and each decaying baryon has exactly the beam energy. Momentum conservation is imposed on the reconstructed baryon-antibaryon pairs by demanding the vector sum of

the total momentum in an event $|\Sigma \vec{\mathbf{p}}|/E_{\text{beam}}$ be less than 0.04. This eliminates background, via $\pi\pi J/\psi$ or $\gamma\chi_{\text{cn}}$ ($n = 0, 1$, and 2), which have extra tracks or showers.

For each baryon-antibaryon candidate event, we calculated the scaled visible energy, E_{vis}/\sqrt{s} , where E_{vis} is the energy observed in an event and \sqrt{s} is the center of mass energy. We define our signal region be $0.98 < E_{\text{vis}}/\sqrt{s} < 1.02$, and two sideband regions of 0.94-0.98 and 1.02-1.06 as representative of the combinatorial background.

We also studied the continuum data to check for a possible contribution to our $\psi(2S)$ signals from this source. This was found to be non-negligible for four of the decay modes as shown in Table I. We multiplied the yield from the continuum data by a scaling factor which was calculated taking into account the differences in luminosity (0.2720), a $1/s^5$ correction (0.9572) for baryons [1], and the values of the efficiencies in the CLEO III and CLEO-c detector configurations before subtracting it from the $\psi(2S)$ yields. This scaling factor was 0.2547 for the $p\bar{p}$ case and similar for the other modes.

Other possible background sources are the daughters from the J/ψ decay combined with the charged or neutral transition pions which can produce possible cross-feed in the signal region. To estimate this cross-feed we generated corresponding Monte Carlo samples of 20,000 events and looked for events which passed our selection criteria for the modes concerned.

Figure 2 shows the scaled energy distribution for each of the decay modes. In all cases, clear signals are seen, with widths as expected from Monte Carlo simulation, and very little combinatorial background in the sideband regions. In each mode we calculate the number of $\psi(2S)$ decays to each final state (“signal yield”) $N_S = S_{\psi(2S)} - B_{\psi(2S)} - S_{xf} - f_s \cdot B_c$ (where $S_{\psi(2S)}$ is the total number of events in the signal region, $B_{\psi(2S)}$ events in the scaled sidebands, S_{xf} is the contribution from the cross-feeds, and $f_s \cdot B_c$ is the scaled continuum contribution with scaled sidebands subtracted). These yields are shown in Table I. The efficiencies, calculated using a weighted average of results from CLEO III and CLEO-c detector simulations, are also shown.

We evaluated the following systematic uncertainties to our measured branching fractions: 3% uncertainty on the number of $\psi(2S)$ decays in our sample; 1% uncertainty in the simulation of our hardware trigger; 1% uncertainty in the reconstruction in each charged track in the event; 1% uncertainty for proton identification of tracks coming from the beamspot, and 2% for proton and kaon identification of tracks coming from the secondary vertices; 1% and 2% uncertainties for photon detection and π^0 reconstruction, respectively; and 1% for background subtraction in $\Lambda\bar{\Lambda}$ mode. The detection efficiency also depends upon the angular distribution of the hyperons. We find a 10% change in efficiency when we change from a flat distribution in $\cos\theta$ to one of the form $1 + \lambda \cos^2\theta$ (where $\lambda = 1$). The value of λ may not be strictly 1 because of effects due to finite charm quark mass [9] and hadron mass effect from $\mathcal{O}(v^2)$ and higher twist corrections to the effective QCD Lagrangian. We compare the detection efficiencies for spin one-half baryon generated samples as discussed above with that obtained by the E835 collaboration [10] and assign the difference, 3.3%, as the systematic uncertainty. We assign a 10% uncertainty in angular distribution to spin 3/2 baryons, which covers all reasonable possibilities. The systematic uncertainty in the hyperon efficiency was estimated from a comparison of the efficiency of the various requirements in a data and Monte Carlo sample. This is largest for the Σ^+ and Ξ^0 modes where the agreement is less satisfactory. In all modes the uncertainty in the reconstruction is doubled as there are two hyperons per event.

Table II displays the breakdown of our systematic uncertainties. The last column tabulates the total systematic uncertainty added in quadrature for each mode.

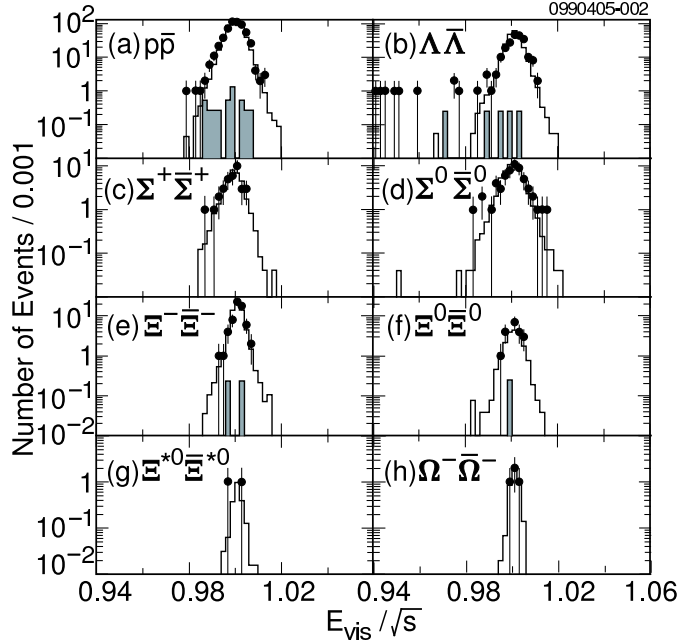


FIG. 2: Scaled energy (E_{vis}/\sqrt{s}) distribution for eight $\psi(2S)$ decay modes: (a) $p\bar{p}$, (b) $\Lambda\bar{\Lambda}$, (c) $\Sigma^+\bar{\Sigma}^+$, (d) $\Sigma^0\bar{\Sigma}^0$, (e) $\Xi^-\bar{\Xi}^-$, (f) $\Xi^0\bar{\Xi}^0$, (g) $\Xi^{*0}\bar{\Xi}^{*0}$, and (h) $\Omega^-\bar{\Omega}^-$. Signal Monte Carlo, data, and scaled continuum plots are shown in solid line, error bar, and filled histograms, respectively.

TABLE I: Branching ratios of $\psi(2S)$ decaying to baryon-antibaryon pairs. The second, third, fourth, and fifth columns show the yields in the signal region, scaled sidebands, scaled continuum, and cross-feeds, respectively. The sixth and seventh columns tabulate the efficiencies and the measured branching fractions, respectively. We used Poisson statistics in evaluating the upper limits on the $\Xi^{*0}\bar{\Xi}^{*0}$ and $\Omega^-\bar{\Omega}^-$ branching fractions @90CL. The eighth column shows the ratio of $\psi(2S)$ to J/ψ decays with statistical and systematic uncertainties added in quadrature. The last column shows the background subtracted continuum cross-section and the systematic error includes 7% due to initial and final state radiation effects and 1% luminosity uncertainty (replacing the uncertainty on the number of $\psi(2S)$ decays).

Modes	$S_{\psi(2S)}$	$B_{\psi(2S)}$	$f_S \cdot B_c$	B_{xf}	ϵ	$\mathcal{B}(10^{-4})$	Q(%)	$\sigma_{\text{cont}}(\text{pb})$
$p\bar{p}$	557	0.5	4.06	0	66.6%	$2.87 \pm 0.12 \pm 0.15$	13.6 ± 1.1	$1.5 \pm 0.37 \pm 0.13$
$\Lambda\bar{\Lambda}$	208	4.5	0.86	0	20.1%	$3.28 \pm 0.23 \pm 0.25$	25.2 ± 3.5	<2.0 @90 CL
$\Sigma^+\bar{\Sigma}^+$	35	0.5	0	0.3	4.1%	$2.57 \pm 0.44 \pm 0.68$	-	-
$\Sigma^0\bar{\Sigma}^0$	58	0	0	0	7.2%	$2.63 \pm 0.35 \pm 0.21$	20.7 ± 4.2	-
$\Xi^-\bar{\Xi}^-$	63	0	0.46	0	8.6%	$2.38 \pm 0.30 \pm 0.21$	13.2 ± 2.2	<3.5 @90 CL
$\Xi^0\bar{\Xi}^0$	19	0	0.49	0	2.4%	$2.75 \pm 0.64 \pm 0.61$	-	<14 @90 CL
$\Xi^{*0}\bar{\Xi}^{*0}$	2	0	0	0.6	0.6%	$0.72_{-0.62}^{+1.48} \pm 0.10$ (<3.2 @90 CL)	-	-
$\Omega^-\bar{\Omega}^-$	4	0	0	0	1.9%	$0.70_{-0.33}^{+0.55} \pm 0.10$ (<1.6 @90 CL)	-	-

TABLE II: Breakdown of systematic uncertainty (%) mode by mode. The last column tabulates the total systematic uncertainty added in quadrature.

Modes	# $\psi(2S)$	Bkg.	Sub.	Trigger	Tracking	Particle ID	Hyperon	π^0/γ	Ang.	Dist.	Total
$p\bar{p}$	3	-	1	2×1.0	2×1	-	-	-	3.3	4.2	
$\Lambda\bar{\Lambda}$	3	1	1	4×1.0	2×2	2×1.0	-	-	3.3	7.7	
$\Sigma^+\bar{\Sigma}^+$	3	-	1	2×1.0	2×2	2×12.8	2×2	3.3	26.5		
$\Sigma^0\bar{\Sigma}^0$	3	-	1	4×1.0	2×2	2×1.5	2×1	3.3	8.1		
$\Xi^-\bar{\Xi}^-$	3	-	1	6×1.0	2×2	2×1.5	-	3.3	9.0		
$\Xi^0\bar{\Xi}^0$	3	-	1	4×1.0	2×2	2×10.5	-	3.3	22.2		
$\Xi^{*0}\bar{\Xi}^{*0}$	3	-	1	8×1.0	2×2	2×2.0	-	10	14.4		
$\Omega^-\bar{\Omega}^-$	3	-	1	6×1.0	$2 \times 2+2 \times 2$	2×2.0	-	10	15.0		

In Table I, we show the measured branching fractions of $\psi(3686)$ decays to baryon-antibaryon modes. The branching fractions for octet baryons are in the range of 0.02 - 0.035 %. Our measured branching fractions for hyperon modes are \sim 50% higher than those in the PDG [4] which are based on lower statistics (12 and 8 events in the Ξ^- and Σ^0 modes, respectively). We note that isospin partners, Σ^+ and Σ^0 and also Ξ^- and Ξ^0 , have similar branching ratios in agreement with naive expectations. Furthermore, we note that addition of strangeness does not greatly change the branching fraction, demonstrating the flavor symmetric nature of gluons. The eighth column in Table I shows the ratio of these $\psi(2S)$ results to those from J/ψ measurements [4]. Two of the results follow the 12% rule closely, but two of them differ by approximately a factor of two. The last column in Table I shows the background subtracted continuum cross-section at $\sqrt{s} = 3.67$ GeV. We quote upper limits @90CL for the $\Lambda\bar{\Lambda}$, $\Xi^-\bar{\Xi}^-$, and $\Xi^0\bar{\Xi}^0$ production in continuum, owing to marginal signal. A 20% correction (upward) is included to account for the initial state radiation [11].

In conclusion, we have analyzed CLEO III and CLEO-c $\psi(3686)$ data corresponding to 3.08×10^6 $\psi(3686)$ decays. We have presented the first observation of the $\psi(3686)$ decaying to $\Xi^0\bar{\Xi}^0$ and $\Sigma^+\bar{\Sigma}^+$ final states, and give improved (high statistics) branching ratios for the $\psi(3686)$ decaying to $p\bar{p}$, $\Lambda\bar{\Lambda}$, $\Xi^-\bar{\Xi}^-$, and $\Sigma^0\bar{\Sigma}^0$ modes. We also give new upper limits on $\Xi^{*0}\bar{\Xi}^{*0}$ and $\Omega^-\bar{\Omega}^-$ final states.

We gratefully acknowledge the effort of the CESR staff in providing us with excellent luminosity and running conditions. This work was supported by the National Science Foundation and the U.S. Department of Energy.

[1] G.R. Farrar and R. D. Jackson, Phys. Rev. Lett. **35**, 1416 (1975); B. L. Ioffe, Phys. Lett. B **63**, 425 (1976); A. I. Vainshtein and V. I. Zakharov, Phys. Lett. B **72**, 368 (1978); S. J. Brodsky and G. P. Lepage, Phys. Rev. D **24**, 2848 (1981).

[2] W. S. Hou and A. Soni, Phys. Rev. Lett. **50**, 569 (1983); W. S. Hou, Phys. Rev. D **55**, 6952 (1992); Y. F. Gu and X. H. Li, Phys. Rev. D **63**, 114019 (2001).

[3] BES Collaboration, J. Z. Bai *et al.*, Phys. Rev. D **67**, 052002 (2003); BES Collaboration, J. Z. Bai *et al.*, Phys. Rev. D **69**, 072001 (2004); BES Collaboration, M. Ablikim *et al.*, Phys. Rev. D **70**, 112003 (2004); BES Collaboration, M. Ablikim *et al.*, Phys. Rev. D **70**, 112007

(2004); CLEO Collaboration, N. E. Adam *et al.*, Phys. Rev. Lett **94**, 012005 (2005).

[4] S. Eidelman *et al.*, Phys. Lett. B **592**, 1 (2004).

[5] CESR-c Taskforce, CLEO-c Taskforce, and CLEO-c Collaboration, R. A. Briere *et al.*, Report No. CLNS 01/1742 (revised 10/01), 2001.

[6] G. Viehhauser *et al.*, Nucl. Instrum. Methods A **462**, 146 (2001); D. Peterson *et al.*, Nucl. Instrum. Methods Phys. Res. A **478**, 142 (2002); M. Artuso *et al.*, Nucl. Instrum. Methods A **502**, 91 (2003).

[7] R. Brun *et al.*, CERN Report No. DD/EE/84-1, 1987.

[8] CLEO Collaboration, I. Danko *et al.*, Phys. Rev. D **69**, 052004 (2004).

[9] M. Claudson, S. L. Glashow and M. B. Wise, Phys. Rev. D **25**, 1345 (1982); C. Carimalo, Int. J. Mod. Phys. A **2**, 249 (1987); F. Murgia and M. Melis, Phys. Rev. D **51**, 3487 (1995).

[10] E835 Collaboration, M. Ambrogiani *et al.*, Phys. Lett. D **610**, 177 (2005).

[11] C. M. Carloni Calame *et al.*, in *Proceedings of the Workshop on Hadronic Cross-Section at Low-Energy (SIGHAD03), 8-10 October 2003, Pisa, Italy*, edited by M. Incagli and G. Graziano (Elsevier, Amsterdam, 2004), p. 258.